Robustness of the inverse cascade in two-dimensional turbulence

Chuong V. Tran and John C. Bowman
Department of Mathematical and Statistical Sciences,
University of Alberta, Edmonton, Alberta, Canada, T6G 2G1
(Dated: December 17, 2003; to appear in Physical Review E)

We study quasisteady inverse cascades in unbounded and bounded two-dimensional turbulence driven by time-independent injection and dissipated by molecular viscosity. It is shown that an inverse cascade that carries only a fraction r of the energy input to the largest scales requires the enstrophy-range energy spectrum to be steeper than k^{-5} (ruling out a direct cascade) unless $1-r \ll 1$. A direct cascade requires the presence of an inverse cascade that carries virtually all energy to the largest scales ($1-r \ll 1$). These facts underlie the robustness of the Kolmogorov–Kraichnan $k^{-5/3}$ inverse cascade, which is readily observable in numerical simulations without an accompanying direct enstrophy cascade. We numerically demonstrate an instance where the $k^{-5/3}$ inverse-cascading range is realizable with 79% of the energy injection dissipated within the energy range and virtually all of the enstrophy dissipated in the vicinity of the forcing region. As equilibrium is approached, the respective logarithmic slopes $-\alpha$ and $-\beta$ of the ranges of wavenumbers lower and higher than the forcing wavenumber satisfy $\alpha+\beta \approx 8$. These results are consistent with recent theoretical predictions.

PACS numbers: 47.27.Gs, 47.27.Eq

I. INTRODUCTION

It is commonly believed that the simultaneous conservation of energy and enstrophy by the advective term of the forced two-dimensional (2D) Navier–Stokes equations gives rise to a dual turbulent cascade in the limit of infinite Reynolds number: energy cascades to low wavenumbers (inverse cascade) and enstrophy cascades to high wavenumbers (direct cascade). Kraichnan [1, 2] predicts that the inverse cascade carries virtually all of the energy input to ever-lower wavenumbers, evading viscous dissipation altogether, and the direct cascade carries virtually all of the enstrophy input to a high wavenumber k_ν, where it is dissipated. This dual cascade hypothesis conjectures that the energy spectrum should scale as $k^{-5/3}$ in the energy-cascading range and as k^{-3} in the enstrophy-cascading range, where k is the wavenumber.

The classical view that two-dimensional unbounded turbulence consists of intricately intertwined inverse and direct cascades is widely believed to be valid in the limit of infinite Reynolds number. However, there has been much numerical evidence presented in which an inverse cascade is observed in the absence of a direct enstrophy cascade [3–6]. This has been attributed to the low Reynolds numbers resolvable by current computers. Recently, Tran and Bowman [7] nevertheless argued on theoretical grounds that an inverse cascade in the absence of an accompanying direct enstrophy cascade is indeed possible for a wide range of Reynolds numbers.

Let us say that an inverse cascade that carries a fraction r of the energy input to the largest scales is *strong* if $1-r \ll 1$; otherwise, the inverse cascade is *weak*. We will show that a weak inverse cascade can never be accompanied by a direct cascade and the small-scale spectrum is required to be steeper than k^{-5}. A direct cascade (if realizable) would require a strong inverse cascade, one that carries virtually all energy to the largest scales. These results provide a theoretical explanation for the robustness of the Kolmogorov–Kraichnan $k^{-5/3}$ inverse cascade, which is readily observable both in numerical simulations (before the energy reaches the lower spectral boundary), and in laboratory experiments, in contrast to the elusive k^{-3} enstrophy cascade [8–10]. Even in the limit of a strong inverse cascade, spectra significantly shallower than k^{-5} in the enstrophy range cannot be guaranteed.

A steady-state enstrophy cascade was recently shown by Tran and Shepherd [11] to be impossible in a bounded domain for an energetically localized forcing. In that case the inverse cascade strength r vanishes. The present work addresses the question of what happens either in an unbounded domain or in bounded quasi-steady flows, before statistical equilibrium is reached. The strength of the inverse cascade is again the key quantity.

We then use a numerical simulation to illustrate that the $k^{-5/3}$ spectrum persists even when most of the energy injection is dissipated in the vicinity of the forcing region, allowing only a small fraction of the energy input to be transferred (*via* a scale-independent energy flux) to the largest scales. Finally, we investigate the dynamical behavior after the inverse cascade reaches the lowest wavenumber. In accord with the constraint derived in [7], no Bose condensation [12] of energy on the largest scale occurs; instead, the $k^{-5/3}$ range gradually steepens as an equilibrium is approached. Note that we discuss only the pure two-dimensional incompressible Navier–Stokes equation, without the addition of any *ad hoc* large-scale damping, unlike most inverse cascade simulations reported in the literature [3, 4, 10, 13].

II. THEORETICAL CONSIDERATIONS

The 2D Navier–Stokes equations governing the motion of an incompressible fluid can be written in terms of the stream function ψ:

$$\partial_t \Delta\psi + J(\psi, \Delta\psi) = \nu\Delta^2\psi + f. \tag{1}$$

The fluid velocity $\boldsymbol{v}$ is given in terms of ψ by $\boldsymbol{v} = (-\partial_y\psi, \partial_x\psi)$. The spatial operators $J(\cdot,\cdot)$ and Δ are, respectively, the 2D Jacobian and Laplacian. The molecular viscosity coefficient is denoted by ν and f represents external forcing. The ensemble-averaged energy spectrum $E(k)$, which represents the energy density associated with the wavenumber k, is defined by

$$E(k) = \frac{1}{2}k^2 \int_{|\boldsymbol{p}|=k} \langle|\widehat{\psi}(\boldsymbol{p})|^2\rangle \, d\boldsymbol{p}, \tag{2}$$

where $\langle\cdot\rangle$ denotes an ensemble average, $\widehat{\psi}(\boldsymbol{p})$ is the Fourier transform of ψ, and the integral is over all wavevectors $\boldsymbol{p}$ having magnitude k. The evolution of the energy spectrum $E(k)$ is governed by (see [1, 14])

$$\frac{d}{dt}E(k) = T(k) - 2\nu k^2 E(k) + F(k). \tag{3}$$

Here $T(k)$ and $F(k)$ are, respectively, the ensemble-averaged energy transfer and energy input rate. The transfer function $T(k)$ satisfies, by virtue of energy and enstrophy conservation,

$$\int_0^\infty T(k)\, dk = \int_0^\infty k^2 T(k)\, dk = 0. \tag{4}$$

The total energy density $E = \int_0^\infty E(k)\, dk$ and enstrophy density $Z = \int_0^\infty k^2 E(k)\, dk$ evolve according to

$$\frac{d}{dt}E = -2\nu Z + \epsilon, \tag{5}$$

$$\frac{d}{dt}Z = -2\nu P + s^2\epsilon, \tag{6}$$

where $\epsilon = \int_0^\infty F(k)\, dk > 0$ is the energy injection rate, $P = \int_0^\infty k^4 E(k)\, dk$ is the palinstrophy density, and s is the forcing wavenumber defined by $s^2 \int_0^\infty F(k)\, dk = \int_0^\infty k^2 F(k)\, dk$. We consider the quasisteady dynamics, where a steady spectrum has been established down to a wavenumber $k_0 \ll s$. The enstrophy is in equilibrium and the energy continues to cascade toward wavenumbers $k < k_0$ at a steady growth rate $dE/dt = \epsilon_0$. It follows from (5) and (6) that

$$\frac{P}{Z} = s^2 \frac{\epsilon}{\epsilon - \epsilon_0}. \tag{7}$$

A direct enstrophy cascade requires $P/Z \gg s^2$ [11], which in turn requires $\epsilon_0 \approx \epsilon$. For a more quantitative analysis, let us assume that the quasisteady spectrum can be approximated by

$$E(k) = \begin{cases} ak^{-\alpha} & \text{if } k_0 \le k < s, \\ bk^{-\beta} & \text{if } s \le k \le k_\nu, \end{cases} \tag{8}$$

where a, b, α, β are constants and k_ν is the highest wavenumber in the enstrophy range, beyond which the spectrum is supposed to be steeper than $k^{-\beta}$. Following [7] we estimate the ratio P/Z as

$$\begin{aligned} \frac{P}{Z} &\ge \frac{a\int_{k_0}^{s} k^{4-\alpha}\, dk + b\int_{s}^{k_\nu} k^{4-\beta}\, dk}{a\int_{k_0}^{s} k^{2-\alpha}\, dk + b\int_{s}^{\infty} k^{2-\beta}\, dk} \\ &= \frac{as^{5-\alpha}\int_{k_0/s}^{1} \kappa^{4-\alpha}\, d\kappa + bs^{5-\beta}\int_{s/k_\nu}^{1} \kappa^{\beta-6}\, d\kappa}{as^{3-\alpha}\int_{k_0/s}^{1} \kappa^{2-\alpha}\, d\kappa + bs^{3-\beta}\int_{0}^{1} \kappa^{\beta-4}\, d\kappa} \\ &= s^2 \frac{\int_{k_0/s}^{1} \kappa^{4-\alpha}\, d\kappa + \int_{s/k_\nu}^{1} \kappa^{\beta-6}\, d\kappa}{\int_{k_0/s}^{1} \kappa^{2-\alpha}\, d\kappa + \int_{0}^{1} \kappa^{\beta-4}\, dk}, \end{aligned} \tag{9}$$

where the inequality results on dropping from the numerator the spectral contribution beyond k_ν (which is considerable if $\beta \le 5$) and the second line is obtained by making the respective changes of variables $\kappa = k/s$ and $\kappa = s/k$ in the two integrals in each of the numerator and denominator. The continuity relation $as^{-\alpha} = bs^{-\beta}$ was used to obtain the third line. It follows that

$$\frac{\int_{s/k_\nu}^{1} \kappa^{\beta-6}\, d\kappa}{\int_{k_0/s}^{1} \kappa^{2-\alpha}\, d\kappa + \int_{0}^{1} \kappa^{\beta-4}\, dk} \le \frac{\epsilon}{\epsilon - \epsilon_0}. \tag{10}$$

Now $\beta = 5$ implies that the dissipation of enstrophy is uniformly distributed among the wavenumber octaves higher than the forcing wavenumber s. A direct cascade requires $\beta < 5$. We consider the non-cascading case $\beta > 5$. If the Kolmogorov–Kraichnan energy-range spectrum ($\alpha = 5/3$) is realizable, the denominator on the left-hand side of (10) is less than $5/4$. On the other hand, the numerator can be considerably larger than $5/4$, making the left-hand side of (10) considerably larger than unity. This requires ϵ_0 to be sufficiently close to ϵ, allowing for the possibility of a strong inverse cascade in the absence of a direct cascade [7]. In order for β to approach 5 from above, (10) requires $\epsilon_0 \to \epsilon$. When $\alpha = 5/3$ and $\beta = 5$, a good lower bound, namely $(4/5)\ln(k_\nu/s)$, for the left-hand side of (10) can be obtained by replacing the lower integration limit k_0/s by 0. For example, if the k^{-5} spectrum extends for five decades of wavenumbers, the left-hand side of (10) must be approximately ten. Therefore, (10) requires $\epsilon_0/\epsilon \approx 0.9$, corresponding to an inverse cascade carrying 90% of the energy input to the largest scales. This explains the robustness of the inverse cascade observed in numerical simulations, regardless of what happens to the enstrophy: in the limit $s/k_\nu \to 0$, as is the case for high-Reynolds number turbulence, any spectral slope $\beta \in (3, 5]$ would require $\epsilon_0 \to \epsilon$. In other words, a direct enstrophy cascade associated with a spectrum even slightly shallower than k^{-5} is ruled out, except

possibly in the limit $\epsilon_0 \to \epsilon$. (The classical enstrophy cascade requires a huge value for the ratio $\epsilon/(\epsilon - \epsilon_0)$.) It is interesting to note that several other theories of 2D Navier–Stokes turbulence predict different values of β in the range $3 < \beta < 5$ [15–17].

Further analytical considerations of (10) are met with difficulties since it is not known how ϵ_0, β, and k_ν vary with Reynolds number. On the other hand, numerical studies of this problem face an equally formidable task (see [7] for a discussion of the numerical limitations). A plausible possibility is to explore how ϵ_0, β, and k_ν adjust with respect to Reynolds number in the non-direct-cascading regime. This information may then be extrapolated to the limit $\beta \to 5$.

III. NUMERICAL RESULTS

We now consider results from simulations that illustrate the realization of an inverse cascade where energy is transferred to the large scales *via* the Kolmogorov–Kraichnan spectrum $k^{-5/3}$, in the absence of a direct cascade. We simulate (1) in a doubly periodic square of side 2π, where the forcing $\widehat{f}(\boldsymbol{k})$ is nonzero only for those wavevectors $\boldsymbol{k}$ having magnitudes lying in the interval $K = [99, 101]$:

$$\widehat{f}(\boldsymbol{k}) = \frac{\epsilon}{N} \frac{\widehat{\psi}(\boldsymbol{k})}{\sum_{|\boldsymbol{p}|=k} |\widehat{\psi}(\boldsymbol{p})|^2}. \tag{11}$$

Here $\epsilon = 0.01$ is the constant energy injection rate and N is the number of distinct wavenumbers in K. The (constant) enstrophy injection rate is $s^2\epsilon \approx 100$, where $s^2 \approx 10^4$ is the mean of k^2 over K. This forcing is described for the velocity formulation in [11]. A similar type of forcing was used by Shepherd [18] in numerical simulations of a large-scale zonal jet on the so-called beta-plane. The attractive aspect of (11), as noted in [18], is that it is steady. We ran dealiased 1365^2 pseudospectral simulations (2048^2 total modes) with $\nu = 5 \times 10^{-5}$. We initialized the simulation with the spectrum $E(k) = 10^{-5}\pi k/(10^4 + k^2)$. Figure 1 shows the evolution of the total energy, enstrophy, and palinstrophy. The dissipation of enstrophy $2\nu P$ quickly reaches the enstrophy injection rate $s^2\epsilon$ (before $t = 10$), giving rise to a quasisteady enstrophy $Z \approx 79$. This amounts to an energy dissipation rate $2\nu Z \approx 0.0079$, accounting for 79% of the energy injection rate. The energy growth rate is then 21% of the energy injection rate, due to the inverse cascade carrying 21% of the energy injection to the lowest wavenumbers. It is evident from the spectrum (time-averaged from $t = 59$ to $t = 60$) in Fig. 2 that the inverse cascade reaches the lowest wavenumber at $t \approx 60$; one observes an energy-cascading range, extended for almost two decades of wavenumbers, with the Kolmogorov–Kraichnan exponent $-5/3$. This is realizable in the complete absence of a direct cascade: the enstrophy range is as steep as $k^{-5.7}$, so that virtually all of the enstrophy is dissipated in the vicinity of the forced region.

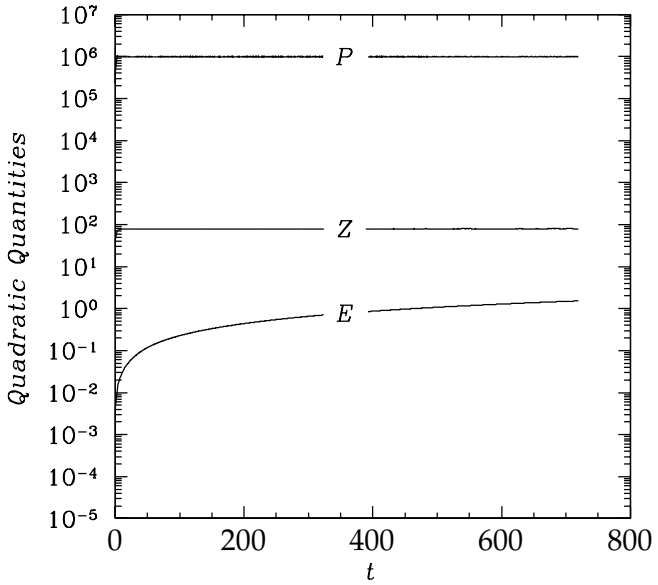

FIG. 1: The energy E, enstrophy Z, and palinstrophy P *vs.* t.

The cumulative energy transfer function $\Pi_E(k) = \int_k^\infty T(p)\, dp$ averaged from $t = 35$ to $t = 60$ is plotted *vs.* k in Fig. 3, along with the cumulative forcing/dissipation $\epsilon_E(k) = \int_k^\infty [2\nu k^2 E(p) - F(p)]\, dp$. The quasisteady nature of the spectrum is reflected in the near coincidence of these two curves for $k > 5$. The energy flux is seen to be nearly uniform between $k = 5$ and $k = 10$; this is a signa-

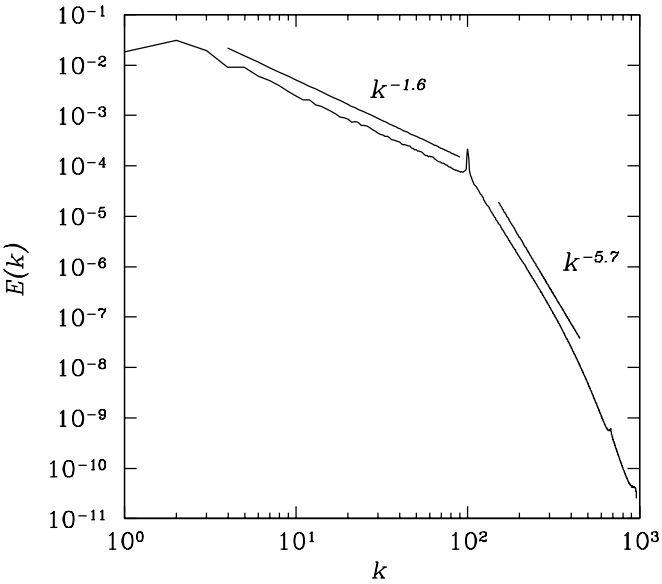

FIG. 2: The energy spectrum $E(k)$ *vs.* k at $t = 60$.

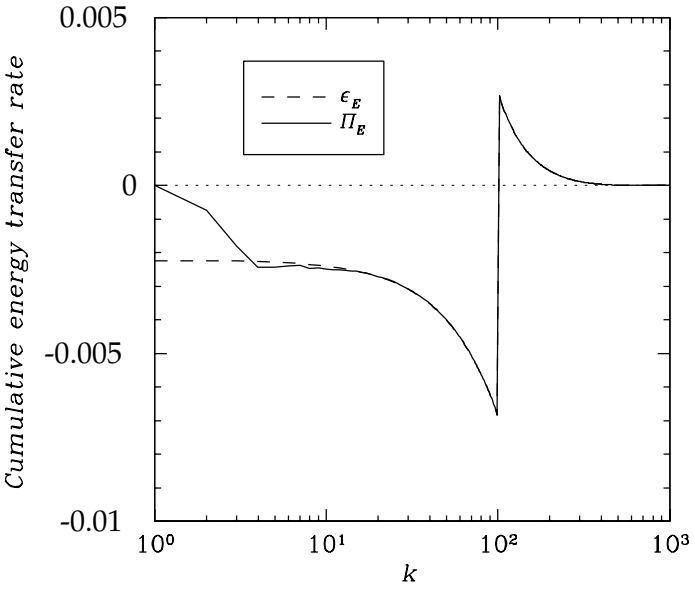

FIG. 3: The cumulative energy transfer function $\Pi_E(k)$ and cumulative forcing/dissipation $\epsilon_E(k)$ *vs.* k averaged between $t = 35$ and $t = 60$.

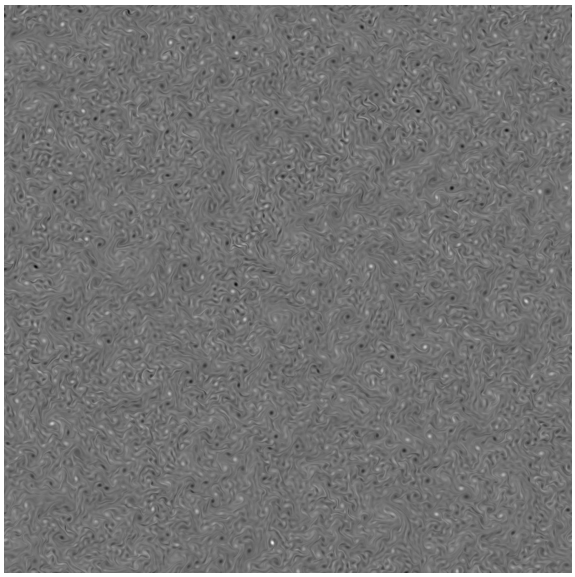

FIG. 4: Vorticity field corresponding to the simulation in Fig. 1 at $t = 28$.

ture of an energy inertial range. Note that $\epsilon_E(k_0) = -\epsilon_0$.

In the corresponding vorticity field, depicted at $t = 28$ in Fig. 4, one notes that the coherent structures in this flow are limited in size to the scale $2\pi/s$ by the decorrelating effect of the forcing. Indeed, since the inverse cascade spectrum is shallower than k^{-3} and the enstrophy-range spectrum is steeper than k^{-3}, one sees immediately that most of the enstrophy must be distributed (in the form of coherent structures) around the forcing scale. In accord with Ref. 11, the forcing scale is also the region of maximum enstrophy dissipation (the spectrum is steeper than k^{-5}).

The above simulation was continued up to $t = 720$, considerably long after the inverse cascade reached the lowest wavenumber (cf. Figure 5). It was observed that the energy growth in the two-decade energy range was just sufficient to allow a spectral slope ≈ -3 to form in the lowest wavenumber decade. A similar result was observed and physically interpreted by Borue [4]. The other decade in the energy range maintained a slope of about $-5/3$ and the enstrophy range remained steady. After that the whole energy range seems to relax toward a slope between -3 and $-5/3$. Since the dissipation rate at the lowest wavenumber, 1, is $2\nu = 10^{-4}$, for the system to approach equilibrium, it would take a time $t \approx 1/(2\nu) = 10^4$ from the moment the inverse cascade reaches wavenumber 1. Nevertheless, the quasisteady assumption that the spectrum from the forcing wavenumber ($s = 100$) to the upper truncation wavenumber ($k_T = 682$) is in equilibrium may be used to predict the final energy-range exponent α. Given that the total equilibrium enstrophy is $\epsilon/2\nu = 100$ and that the enstrophy contribution $Z(k > k_1) = 38.4$ from wavenumbers larger than $k_1 = 90$ has already reached equilibrium, the remaining enstrophy contribution must come from the large scales: $100 - 38.4 = E(k_1) \int_1^{k_1} k^2 (k/k_1)^{-\alpha}\, dk$. We measured $E(k_1) = 8.2 \times 10^{-5}$ and used this value to deduce that the exponent α of an equilibrium energy range extending from $k_0 = 1$ to k_1 must be 2.04. It follows that $\alpha + \beta \approx 8$, in rough agreement with the result $\alpha + \beta \geq 8$ derived in [7] on the basis of the balance equation $P = s^2 Z$ [obtained by setting $\epsilon_0 = 0$ in (7)] for a bounded fluid in equilibrium, with $k_\nu/s \geq s/k_0$. In the present case, we have $k_\nu/s \approx 5$ and $s/k_0 \approx 100$, so that the condition $k_\nu/s \geq s/k_0$ is violated; this allows the sum $\alpha + \beta$ to fall slightly below eight. In order to obtain $k_\nu/s \geq s/k_0$ one would have to extend k_ν to at least 10^4.

Finally, we note that in a bounded domain, a k^{-3} enstrophy cascade can in fact be obtained if one includes a linear damping at the large scales. This breaks the balance equation $P = s^2 Z$ and the constraint $\beta > 5$ derived from it [11], allowing the k^{-3} enstrophy cascade illustrated in Fig. 6 to form (dashed curve, with $\sqrt{P/Z} \approx 20 \gg s = 2$). If one in addition artificially sets the molecular dissipation to zero within the enstrophy inertial range by introducing the cutoff $k_H = 300$, one obtains the pristine logarithmically corrected inertial range depicted in Fig. 6 [19] (solid curve, with $\sqrt{P/Z} \approx 65 \gg s = 2$). Given an energetically localized forcing, these direct enstrophy cascades have been proven to be unrealizable in a steady state when the (Laplacian) molecular viscosity acts alone [11].

The vorticity fields corresponding to the spectra in Fig. 6 are shown in Figs. 7 and 8. The fact that fewer coherent structures are seen in Figs. 7 and 8 than in Fig. 4

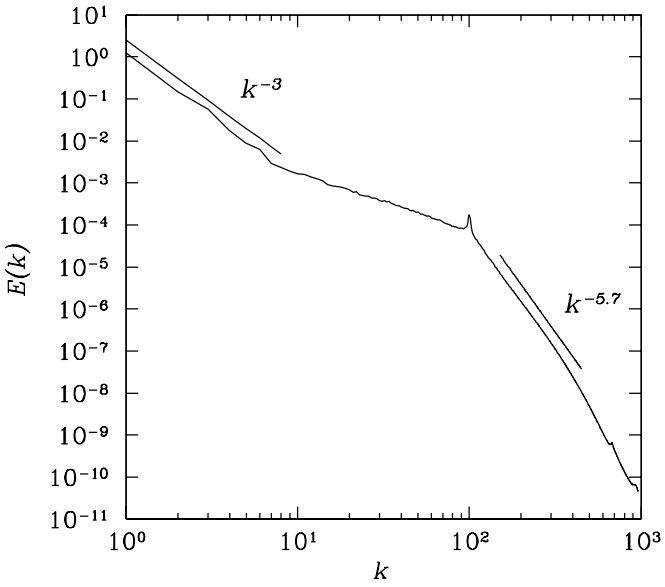

FIG. 5: The energy spectrum $E(k)$ *vs.* k at $t = 720$.

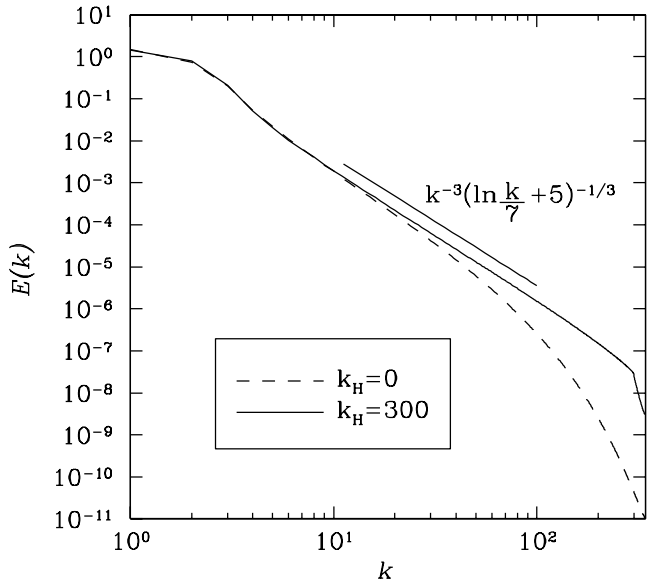

FIG. 6: Direct enstrophy cascades (683^2 dealiased modes) forced at wavenumber 2, with small-scale molecular dissipation coefficient $1.25 \times 10^{-4} k^2 H(k - k_H)$ (H denotes the Heaviside function) and large-scale dissipation coefficient $0.1k^0$ for $k \leq 3$.

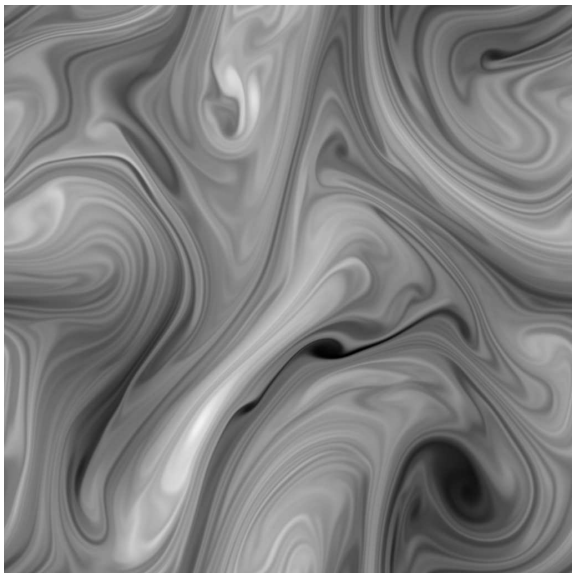

FIG. 7: Vorticity field corresponding to the simulation in Fig. 6 with $k_H = 0$.

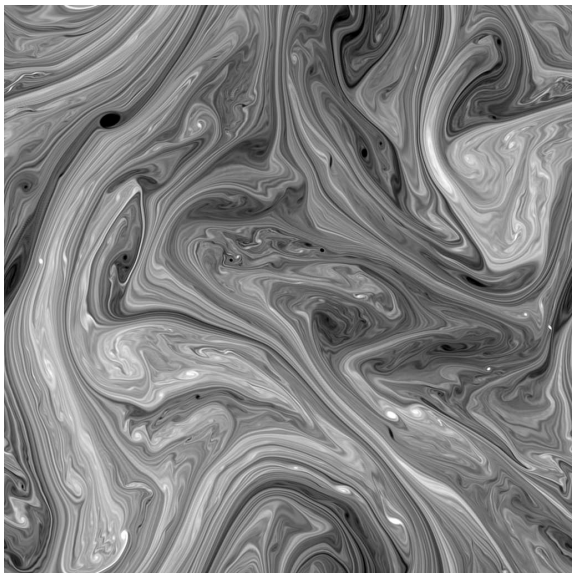

FIG. 8: Vorticity field corresponding to the simulation in Fig. 6 with $k_H = 300$.

supports the suggestion [20] that coherent structures are associated with steep enstrophy-range spectra. However, these steep spectra were shown in Refs. 7 and 11 to be a consequence of the global properties of a bounded fluid, and it may well be that it is the steepness of the spectrum (steeper than k^{-5}) that allows the coherent structures seen in Fig. 4 to form, rather than the other way around.

Ultimately, to settle the question about the validity of the Kraichnan theory of the dual cascade, it will be necessary to learn more about the behavior of the inverse cascade strength $r = 1 - 2\nu Z/\epsilon$ with Reynolds number R. The variation of r with t is shown in Fig. 9 for a series of runs based on the simulation presented in Fig. 1, formed by scaling s and the number of modes in each direction by λ and ν by $1/\lambda^2$, for $\lambda = \{1/8, 1/4, 1/2, 1, 2\}$. A well-developed $k^{-5/3}$ quasisteady inverse cascade forms only for the three highest resolutions in this series. In Fig. 10 we illustrate the behavior thus obtained for r *vs.* the steady-state Reynolds number $(2\pi/s)^2\sqrt{Z}/\nu = (2\pi/s)^2\sqrt{\epsilon/(2\nu)}/\nu$ determined

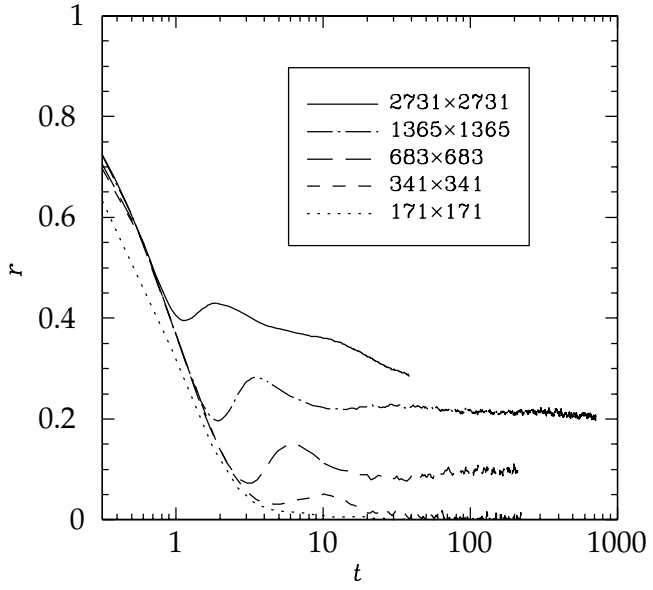

FIG. 9: Inverse cascade strength *vs.* t for several dealiased resolutions.

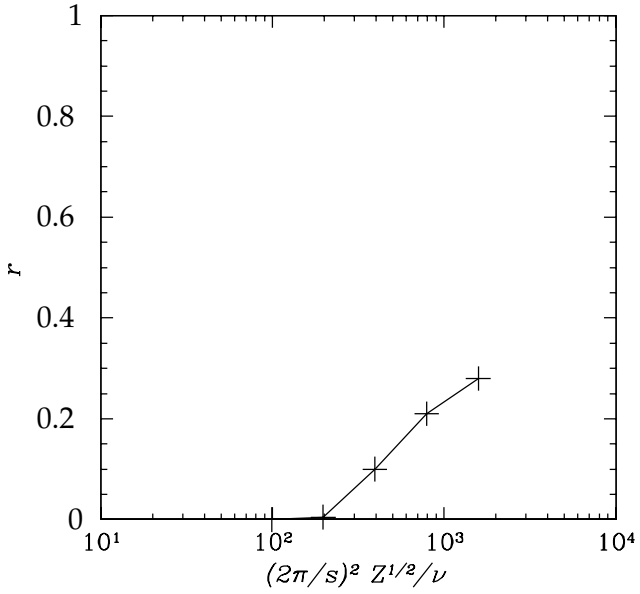

FIG. 10: Inverse cascade strength *vs.* Reynolds number.

by (5). We note that the inverse cascade strength certainly increases with Reynolds number, as expected, but what happens in the high-Reynolds number limit remains unclear. As seen from (7), the manner in which the palinstrophy diverges as the Reynolds number increases is critical to the validity of the dual cascade theory. What is clear is that our highest resolution is still far away from being able to assess this theory. Even if the inverse cascade strength should continue to rise with the roughly linear dependence (with respect to the logarithm of the Reynolds number) suggested in Fig. 10, at least two more decades in Reynolds number would be needed at this rate to reach the strong inverse cascade regime ($r = 1$) required for the existence of a quasisteady direct enstrophy cascade.

IV. DISCUSSION

In conclusion, we have derived a relation, (10), between the energy growth rate, the enstrophy-range spectral slope, and the dissipation wavenumber. We used this to explain how an inverse cascade can be realizable in the complete absence of a direct cascade, as observed in direct numerical simulations reported in the literature.

An inverse energy cascade transferring energy to the large scales *via* the Kolmogorov–Kraichnan spectrum $k^{-5/3}$ and an enstrophy range significantly steeper than k^{-5} form, consistent with many numerical results in the literature, in which large-scale long-lived vortices, known as coherent structures, are observed [4, 20–25]; these are often blamed for causing enstrophy spectra steeper than k^{-3}. However, these steep spectra can be explained without reference to coherent structures: the steepness is merely a consequence of global conservation laws, molecular viscosity, and a spectrally localized forcing [7, 11].

The inverse cascade is seen to carry only a small fraction of the energy input to the largest scale and yet a $k^{-5/3}$ spectrum manifests itself nonetheless. This suggests that a $k^{-5/3}$ inverse-cascading range does not require the transfer of virtually all energy input to the largest scales in the system. We ran our numerical simulations significantly long after the inverse cascade reached the lowest wavenumber and observed the subsequent approach to equilibrium. We noticed that the energy-range spectral slope gradually steepens in accord with the constraint $P = s^2 Z$ for equilibrium dynamics. The results reported here are thus consistent with recent theoretical analyses [7, 11].

Equation (7) establishes that a direct cascade cannot coexist with a weak inverse cascade. This feature is common to a general class of incompressible fluid turbulence in two dimensions known as α turbulence [26] and not limited to the present case. Turbulence in a bounded domain will eventually approach an equilibrium state [12], with $\epsilon_0 = dE/dt = 0$. We thus recover a principal result from Refs. 7 and 11: any (bounded) numerical simulation of the two-dimensional incompressible Navier–Stokes equation cannot exhibit a direct cascade in equilibrium. Numerical inverse cascades in the existing literature, limited by finite resolution, are inherently weak; (7) implies that these weak inverse cascades cannot be accompanied by a k^{-3} enstrophy-range spectrum; in fact, the spectrum must be steeper than k^{-5}. A direct cascade is ruled out until the inverse cascade becomes extremely strong. In order to gain insight into the realizability of a direct cascade, it may help to develop a detailed understanding of

the dynamics of the critical k^{-5} spectrum that separates the noncascading and direct cascading regimes. Finally, we wish to point out that the fact that an inverse energy cascade at moderate Reynolds numbers carries only a fraction of the injected energy to the largest scales has important implications for accurate estimation of the energy inertial range Kolmogorov constant.

In this work we have established a necessary condition for a direct cascade to be realizable: the inverse cascade strength must approach unity as the Reynolds number is increased. The realization of an inverse cascade in the absence of a direct cascade poses closely related interesting questions that provide excellent topics for further study. First, how does the relative strength of the inverse cascade depend on the Reynolds number? Second, what Reynolds number corresponds to the onset of a direct cascade, if such a threshold exists? While we have made a preliminary attempt at answering the first question, the second question remains completely open for future study.

ACKNOWLEDGMENTS

This work was funded by the Pacific Institute for the Mathematical Sciences and the Natural Sciences and Engineering Research Council of Canada.

[1] R.H. Kraichnan, Phys. Fluids **10**, 1417 (1967).
[2] R.H. Kraichnan, J. Fluid Mech. **47**, 525 (1971).
[3] G. Boffetta, A. Celani, and M. Vergassola, Phys. Rev. E **61** R29 (2000).
[4] V. Borue, Phys. Rev. Lett. **72** 1475 (1994).
[5] D. Fyfe, D. Montgomery, and G. Joyce, J. Plasma Phys. **17**, 369 (1977).
[6] U. Frisch and P.L. Sulem, Phys. Fluids **27** 1921 (1984).
[7] C.V. Tran and J.C. Bowman, Physica D **176**, 242 (2003).
[8] J. Paret and P. Tabeling, Phys. Rev. Lett. 79 4162 (1997).
[9] J. Paret and P. Tabeling, Phys. Fluids 10 3126 (1998).
[10] T. Dubos *et al.*, Phys. Rev. E **64**, 36302 (2001).
[11] C.V. Tran and T.G. Shepherd, Physica D **165**, 199 (2002).
[12] A common misconception is that the energy of the two-dimensional Navier–Stokes in a bounded domain will grow indefinitely, as more and more energy piles up at the largest scale. Boundedness of the energy (for a bounded energy injection rate ϵ) follows immediately on applying the Poincaré inequality to (5); this yields a dissipative first-order differential equation that provides an upper bound on the energy (cf. Ref. [27]).
[13] A. Babiano, B. Dubrulle, and P. Frick, Phys. Rev. E **55**, 2693 (1997).
[14] U. Frisch, Turbulence: The Legacy of A.N. Kolmogorov (Cambridge University Press, Cambridge, 1995).
[15] H.K. Moffatt, Advances in Turbulence, (Springer, Berlin, 1986).
[16] P.G. Saffman, Stud. Appl. Math. **50**, 377 (1971).
[17] P.L. Sulem and U. Frisch, J. Fluid Mech. **72**, 417 (1975).
[18] T.G. Shepherd, J. Fluid Mech. **183**, 467 (1987).
[19] J.C. Bowman, J. Fluid Mech. **306** 167 (1996).
[20] A. Babiano *et al.*, J. Fluid Mech. **183**, 379 (1987).
[21] J.C. McWilliams, J. Fluid Mech. **146**, 21 (1984).
[22] J.C. McWilliams, J. Fluid Mech. **219**, 361 (1990).
[23] P. Santangelo, R. Benzi, and B. Legras, Phys. Fluids A **1** 1027 (1989).
[24] L.M. Smith, V. Yakhot, Phys. Rev. Lett. **71**, 352 (1993).
[25] L.M. Smith, V. Yakhot, J. Fluid Mech. **271**, 115 (1994).
[26] C.V. Tran, Physica D (to be published).
[27] C. Foias *et al.*, Physica D **9** 157 (1983).